

Vibronic energy map and excited state vibrational characteristics of magnesium myoglobin determined by energy-selective fluorescence

ANDRAS D. KAPOS[†] AND JANE M. VANDERKOOI^{*}

^{*}Department of Biochemistry and Biophysics, School of Medicine, University of Pennsylvania, Philadelphia, PA 19104; and [†]Laboratory of Biophysics of the Hungarian Academy of Sciences, Budapest, H1444, Box 263 Hungary

Communicated by Robin M. Hochstrasser, September 8, 1992 (received for review April 30, 1992)

ABSTRACT The vibrational frequencies of the singlet excited state of Mg-substituted myoglobin and relative absorption probabilities were determined by fluorescence line-narrowing spectroscopy. These spectra contain information on the structure of the excited state species, and the availability of vibrationally resolved spectra from excited state biomolecules should aid in elucidating their structure and reactivity.

Reactions occurring from electronically excited state molecules in proteins are important for photosynthesis, as well as for other photochemical reactions involving a large variety of chromophores. The structure of the excited state molecule must be different from that of the ground state molecule, but conventional techniques do not allow us to obtain structural information from short-lived excited state biological macromolecules. In principle, the vibrational levels of the excited state could be obtained from electronic absorption spectra, but for chromophores in proteins these show no vibrational resolution. One reason for this is that proteins have a dynamic structure. This means that when a prosthetic group is embedded in the protein, its environment varies in time, and the environment varies for individual prosthetic groups at a fixed-time glance. For prosthetic groups that are chromophores, the environmental variations cause inhomogeneous broadening of the conventional absorption and emission spectra, which obscures the information on the vibrational levels.

Energy-selective fluorescence, or fluorescence line-narrowing (FLN) technique, one of the "site"-selective spectroscopic methods (1, 2), allows the obtainment of vibrationally resolved fluorescence spectra from inhomogeneously broadened porphyrins in heme proteins (3–5). FLN uses temperatures close to 0 K to assure that the molecules before excitation are in the lowest vibrational level of the ground electronic state and that different surrounding effects remain static. A narrow laser light source is used to select those subsets of molecules which have energy levels from the ground state lowest vibrational level that are equal to the energy of the laser photon. In this paper we describe how FLN spectra can be used to obtain not only a quantitative measure of inhomogeneous broadening but also the vibrational energies of the excited state molecule and the $0, 0 \rightarrow 0, m$ absorption probabilities for a chromophore in a protein. To describe the method we define the use of a vibronic energy map, and we determine the selective excitation spectrum of magnesium protoporphyrin in myoglobin (MgMb).

Materials and Instrumentation

MgMb was prepared from horse myoglobin (Sigma) by combining apomyoglobin and Mg protoporphyrin IX, as described (4). The sample was about 10–50 μ M in porphyrin and

was dissolved in 100 mM phosphate buffer (pH 7.0) with 50% (vol/vol) glycerol. High-resolution fluorescence emission spectra were obtained by using the instrument as described earlier (5). The resolution of the spectrophotometer was about 1 cm^{-1} . The sample was cooled by a liquid helium flow cryostat (APD Cryogenics, Allentown, PA). Conventional fluorescence spectra were obtained on a Perkin-Elmer LS-5 Fluorescence Spectrophotometer equipped with a xenon lamp. The sample was in a quartz dewar filled with liquid nitrogen. Nanosecond fluorescence decay parameters were measured by using a time-correlated single-photon-counting instrument described by Holtom *et al.* (6).

Approximations

The variation of the protein environment is revealed in the deformation of the vibronic structure of the chromophore. Kohler (7) has shown that, to first approximation, the solvent shifts the electronic levels of the solute only, while the corresponding vibrational levels remain the same. The *approximation of pure electronic distortion* holds if (i) the effect of the environment on the chromophore is manifested as a change in the energy gap (E_{gap}) between the first excited electronic and the ground electronic manifolds, while the vibrational structure remains unchanged,

$$E_{0,m} - E_{0,n} = \text{constant}_1 \quad E_{1,m} - E_{1,n} = \text{constant}_2, \quad [1a, 1b]$$

and (ii) the transition probabilities (absorption, A , and fluorescence emission, F) between the ground and the excited state vibronic levels do not vary for molecules having different electronic energy gaps, i.e.,

$$A \neq f(E_{\text{gap}}) \quad F \neq f(E_{\text{gap}}). \quad [2a, 2b]$$

Even with laser excitation and at cryogenic temperatures the vibrational levels are not lines. They consist of a narrow zero phonon line and a broader phonon wing (1, 2). These phonon wings cause a wide background on which the zero phonon lines are superimposed.

Vibronic Energy Map

In a homogeneous environment the members of a set of identical chromophores have the same electronic and vibrational energy structure. The absorption and emission lines are sharp (Fig. 1 A and B) and the situation is illustrated by the Jablonski diagram (Fig. 1C).

If the individual chromophores have different environments that distort uniquely the chromophore, each molecule can have its own energy values, which can be different from those of the other molecules. This situation can be illustrated by a diagram called a vibronic energy map (8). To introduce

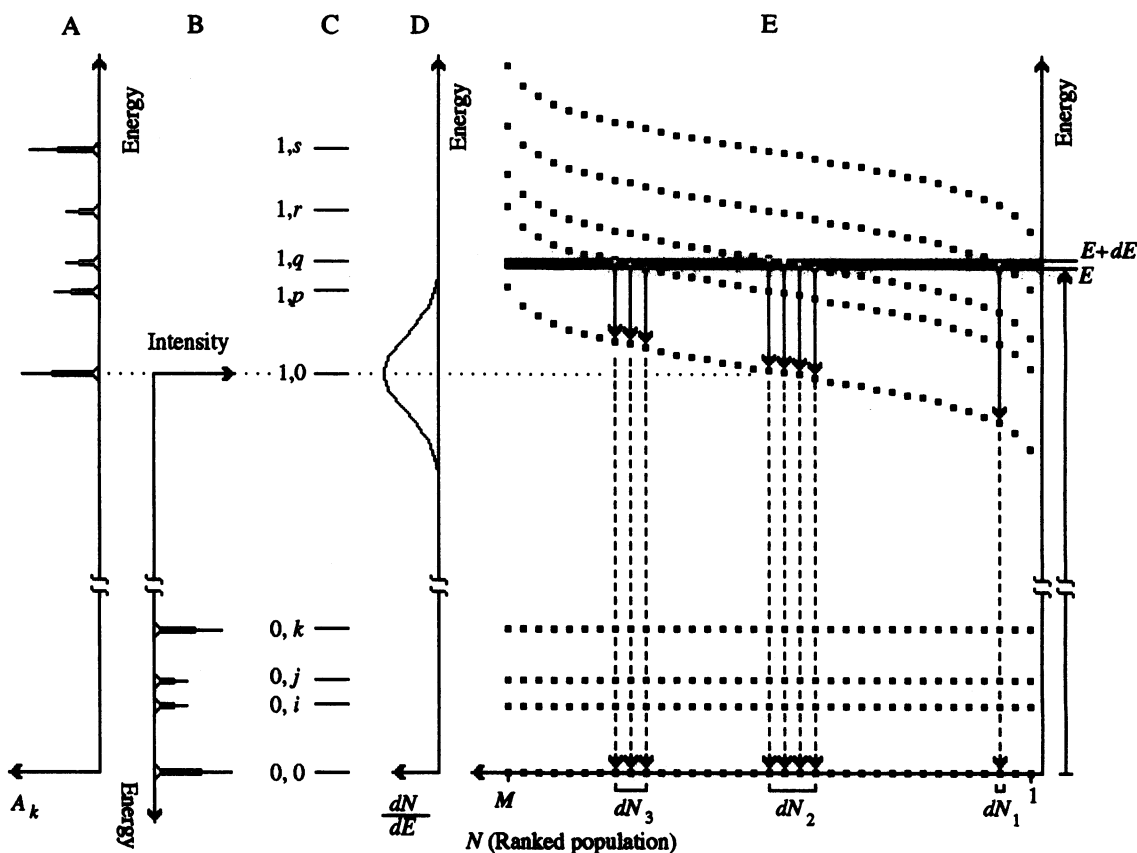


FIG. 1. (A) Idealized absorption spectrum. (B) Idealized emission spectrum. (C) Jablonski diagram. The numbers refer to the different electronic states and vibrational levels. (D) Population distribution function (PDF). (E) Vibronic energy map.

it consider a simple system, for which the approximation of pure electronic distortion is valid and the values of the electronic gap are distributed symmetrically around one characteristic value. The diagram for the vibronic energy map is in Fig. 1E and it is explained as follows. Analogously to the Jablonski diagram, the vibronic energy map has an axis that shows the values for the electronic and vibrational energies of the molecules. Although it is the vertical scale, consider it to be the independent axis. The other axis is the ranked population axis. This horizontal axis is the dependent axis and is directed from right to left. The set of probed molecules with their possible vibronic energy values are ordered according to the electronic energy gap. In Fig. 1E the molecules are in this hierarchical order. The first molecule, with the smallest energy gap, is closest to the energy axis, and the last molecule, which has the biggest energy gap, is furthestmost. The possible electronic and vibrational energy levels are discrete values; therefore, each molecule is represented by a series of such energy values along the energy axis. The range of the horizontal axis spans from 1 to the total number of the molecules (M). The different vibrational values of the electronic ground state ($0, k$) in the approximation 1a form horizontal parallel lines, called vibrational surfaces, on the diagram. According to the approximation in Eq. 1b, the vibrational levels of the first excited electronic state ($1, k$) also form parallel curves (if we measure the distance parallel to the energy axis). In general, molecules with the same electronic gap can have different vibrational energies. In this situation one can use the same convention, letting the preceding molecule be the one which has the smallest vibrational energy.

An extension of the vibronic energy map to three dimensions would show the transition probabilities along the third axis. The k th vibrational surface of the ground electronic state contains the probability of the $1, 0 \rightarrow 0, k$ transitions,

and the m th vibrational surface of the first excited electronic state contains the probabilities of the $0, 0 \rightarrow 1, m$ transitions.

Population Distribution Function

Each of the excited state vibrational surfaces carries information about the population of the molecules with different energy levels. Therefore, any of these curves represents the cumulative population distribution of an inhomogeneously broadened set of molecules.

Remembering that the independent axis is the energy scale, we see that the derivative (dN/dE) of the cumulative population distribution function gives the density function of the distribution of the molecules in the energy scale; in other words, it gives the population distribution function (PDF). If the energy values of the electronic gap are distributed around one characteristic value, the PDF has one peak, as in Fig. 1D.

Based on the work of Fuenfschilling and Zschokke-Graenacher (9), Fidy *et al.* (10) have given an implicit definition of the PDF, also called the inhomogeneous distribution function. A generalized version of this definition is the following:

$$I_m = I_{exc}(dN/dE)A_kV_kF_mK, \quad [3]$$

where I_m is the line intensity of a $1, 0 \rightarrow 0, m$ transition; I_{exc} is excitation intensity; dN/dE is the population distribution function; A_k is the $0, 0 \rightarrow 1, k$ absorption transition probability; V_k is related to the $1, k \rightarrow 1, 0$ vibrational transition probability; F_m is the fluorescence $1, 0 \rightarrow 0, m$ emission probability; and K is an arbitrary constant.

The FLN spectra usually can be divided into two main parts. These are the "pure" $1, 0 \rightarrow 0, 0$ and the "mixed" $1, 0 \rightarrow 0, m$ ($m \neq 0$) regions. For porphyrins, the $1, 0 \rightarrow 0, 0$ region is the more intense, and this was used in our determination.

Consider the situation in Fig. 1E to interpret Eq. 3 for $m = 0$. For a wide range of excitation intensities the $1, 0 \rightarrow 0, 0$ line intensity (I_0) is proportional to the excitation intensity (I_{exc}). The arrow to the right of Fig. 1E shows the excitation energy (E), whose uncertainty (dE) is a small but finite value. As previously demonstrated (1, 11), a single excitation frequency can excite more than one subpopulation of molecules; in Fig. 1E, three subsets of molecules are excited—namely, those which have vibrational levels falling between E and $E + dE$. These subsets are represented by small segments of the vibrational surfaces. In general the number of molecules in each subset is different. The projection of the segments (of the vibrational surfaces) onto the ranked population scale gives the number of molecules in the subset. These values are dN_1 , dN_2 , and dN_3 . I_0 is proportional to dN and inversely proportional to dE , which are together the PDF. If the PDF is a Gaussian function (as in Fig. 1E), the closer the subset is to the mean value of the distribution, the larger the number of molecules in the subset. The absorption probabilities of the various vibrational surfaces (Fig. 1A) are different, but they are constant along one vibrational surface, in accordance with Eq. 2a. The bigger A_k is, the larger the I_0 . The solid arrows in Fig. 1E represent vibrational relaxations, and the fluorescence emission occurs from the lowest vibrational level (1, 0). The $1, 0 \rightarrow 0, 0$ transitions are represented in Fig. 1E by dashed arrows. The measured spectrum is a sum of several subspectra (e.g., a sum of three subspectra in Fig. 1E, if we neglect the small differences within one subspectrum). These subspectra according to Eq. 2b have the same but shifted pattern (Fig. 1B). The distances between the peaks are the same, but the distances between the “first” peak and the 0 value are different for the different subsets. Along with the above parameters I_0 is also proportional to F_0 .

Experimentally the PDF is determined from the spectra by measuring how the intensity of the $1, 0 \rightarrow 0, 0$ emission peak, I_0 , coming from one chosen vibrational surface (e.g., from 1, k) depends on the emitted energy. This means that I_{exc} , V_k , and F_0 in Eq. 3 are constant. I_0 evaluated by this method and the emission energy determine one point of the function (f_k) which is the product of A_k and the PDF:

$$f_k = A_k(dN/dE). \quad [4]$$

For fixed k the function f_k has the same shape as the PDF, which is why it was used earlier as the PDF itself (8, 9).

Absorption Characteristics

From f_k functions (Eq. 4) it is possible to determine both the PDF and the A_k values (7). If Eqs. 1 and 2 are valid, the shapes of different f_k functions are approximately the same. We can get the same PDF function by multiplying the f_k functions by scaling factors. If we ignore an arbitrary multiplication constant, these scaling factors are the reciprocal values of the absorption probabilities (A_k , $k = 1, 2, \dots$).

We introduce another method to describe the absorption probabilities of the vibrational surfaces of the first electronic excited state in the case of an inhomogeneous environment. If we consider the inhomogeneously broadened $1, 0 \rightarrow 0, 0$ region of the fluorescence emission spectra, using the differences between the excitation energy and the fluorescence emission energy as a scale (i.e., the shifted scale), the peak positions give a part of the excited state vibrational energies. According to Fig. 1E three vibrational energies (the length of the solid arrows) can be determined by taking the difference between the excitation energy (the length of the arrow located at right of Fig. 1E) and the $1, 0 \rightarrow 0, 0$ fluorescence emission energy of the individual subsets (the length of the dashed arrows). The spectra at different excitation energies on the shifted scale reveal different parts of the vibrational

energies, and by changing the excitation energy it is possible to determine almost all the excited state vibrational energies. Consider two spectra that contain at least one “common” peak. The position of this peak is the same on the shifted scale, but in general the intensities are not. The reason for these intensity differences is the difference among the numbers of molecules excited for the selected subsets.

We can get the selective excitation spectrum of an inhomogeneously broadened set of molecules, in which the population differences are averaged, if we simply add the $1, 0 \rightarrow 0, 0$ regions of sufficiently high number of fluorescence emission spectra, provided that these spectra are presented on a scale that is shifted relative to the excitation. The difference of the excitation energies between the neighboring spectra should be the same, the value of this difference should be relatively small compared with the width of the PDF, and the spectra should be normalized to the excitation intensity.

Applications

In Fig. 2, a conventional spectrum (at 77 K) and two FLN spectra (at 4.2 K) of MgMb can be compared. The excitation wavelength of the conventional fluorescence spectrum was 557 nm, and the slitwidths of the monochromators were 3 nm, which correspond to the energy range 17,900–18,000 cm^{-1} . The two boundary values of this range, 18,000 and 17,900 cm^{-1} , were the excitation energies of the FLN spectra B and C, respectively. The highly resolved $1, 0 \rightarrow 0, 0$ region (ZPLs) of MgMb is located between 16,600 and 17,040 cm^{-1} . The peaks in that range on B and C represent the excited state vibrational levels from 1056 to 1342 cm^{-1} and from 904 to 1247 cm^{-1} (from right to left). One of them, the 1230 cm^{-1} , is marked with a star. The excited state molecule was further characterized by the fluorescence lifetime, which is about 11 ns at 77 K.

The fluorescence emission of the $1, 0 \rightarrow 0, 0$ transitions (between 16,600 and 17,040 cm^{-1}) was examined by using excitation in the range of 16,850 to 18,190 cm^{-1} . Seven representative spectra with 200- cm^{-1} increments in excitation energy are shown in Fig. 3A. The dotted line in Fig. 3B is the conventional absorption spectrum of MgMb at 77 K, using 655 nm as detection wavelength with 3-nm monochromator slitwidth, which corresponds to the energy range

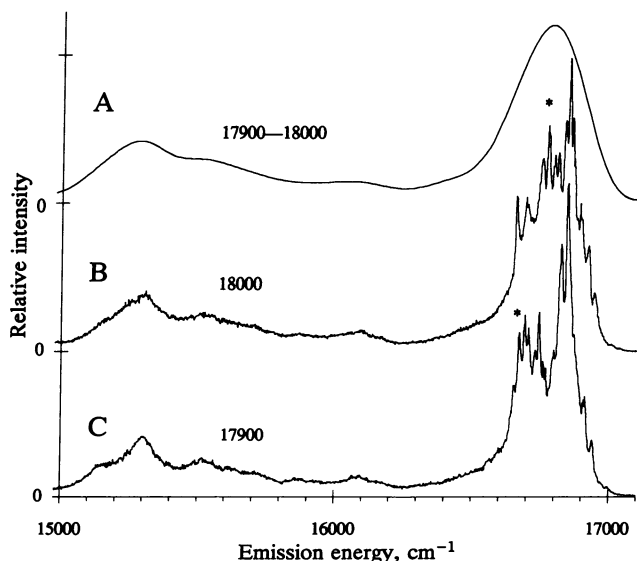


FIG. 2. Conventional emission spectra of MgMb at 77 K (spectrum A) and FLN spectra of MgMb at 4.2 K (spectra B and C). Excitation energies are indicated (cm^{-1}) above the spectra.

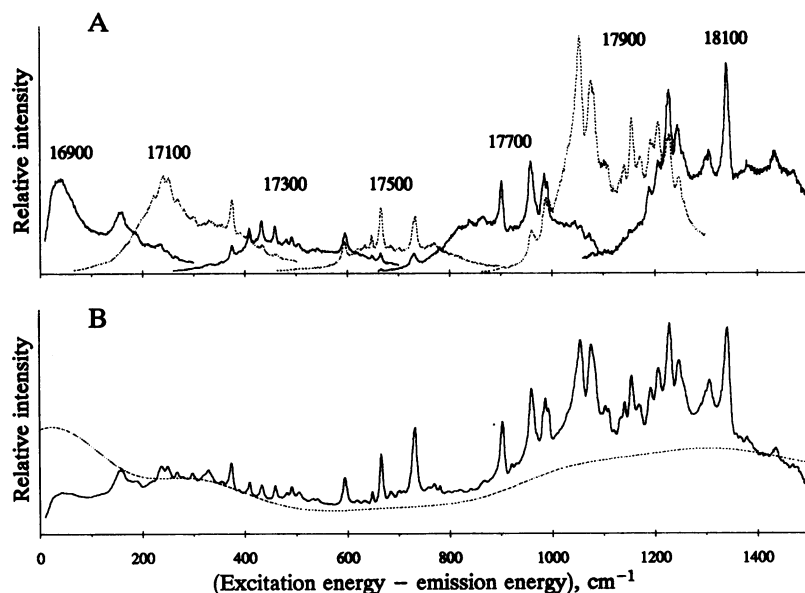


FIG. 3. (A) Shifted FLN spectra at 4.2 K in the $1, 0 \rightarrow 0, 0$ region of MgMb. Excitation energies are indicated (cm^{-1}). (B) Solid line, selective excitation spectrum of MgMb; dotted line, conventional excitation spectrum of MgMb.

$15,230\text{--}15,300\text{ cm}^{-1}$. The scale shows the differences between the excitation energies and the most significant peak of the PDF ($16,870\text{ cm}^{-1}$). The selective excitation spectrum, as the sum of 135 shifted and normalized spectra taken with 10-cm^{-1} increments in excitation energy, is shown in Fig. 3B (solid line). This spectrum accurately gives the vibrational energies of the first electronic excited state and the relative absorption probability, A_k , in the range $190\text{--}1360\text{ cm}^{-1}$. The resolution of the resultant spectrum is high, indicating that the approximation of pure electronic distortion in the case of MgMb is valid to a high degree. It is possible to extend the accurate region of the selective excitation spectrum above 1360 cm^{-1} , since the spectra remain resolved even at excitation above $18,190\text{ cm}^{-1}$. Below 100 cm^{-1} the spectrum shows only a broad feature that probably is due to the phonon wing of the $1, 0$ vibrational surface. The phonon-wing contribution of the $0, 0$ vibrational surface would contribute only

to the background of this spectrum. The method of selective excitation cannot yield the absorption probability of the $1, 0 \rightarrow 1, 0$ excitation and $1, 0 \rightarrow 0, 0$ emission cannot be measured simultaneously.

The PDF was determined by following the peak of the 373-cm^{-1} vibrational level. The distribution was bimodal; we fitted two Gaussian functions to the peaks (Fig. 4B). The mean values of the distribution are $16,720$ and $16,870\text{ cm}^{-1}$, with 53 and 33 cm^{-1} as standard deviations. From the whole emitted intensity, 53% and 47% belong to the two Gaussian functions, respectively. Non-single Gaussian distributions have also been observed in the PDF of Zn mesoporphyrin horseradish peroxidase (12) and metal-free cytochrome c (13). The existence of more than one population for CO-Mb is also inferred from infrared spectroscopy of CO (14, 15). From the data presented in Figs. 3 and 4B, the excited state vibrational surface for MgMb can be constructed. A portion of this is shown in Fig. 4A.

Conclusions

The vibronic energy map describes the vibronic energy structure of an inhomogeneously broadened set of molecules. In the case of pure electronic distortion, the PDF can characterize the distribution of the chromophores in the energy scale, where the PDF is given by the derivative of the $(1, 0)$ vibrational surface in the energy map. By surveying both the excitation and emission energies, we can also obtain the selective excitation spectrum that yields the excited state vibrational energies and relative absorption coefficients of the transitions. The technique should have general applicability to the study of fluorescent biological macromolecules in those cases where inhomogeneous broadening does contribute significantly to the overall broadening.

We thank Drs. J. Fidy and V. Logovinsky for valuable discussions. This work was supported by U.S. National Science Foundation Grant DM-88-15723.

1. Personov, R. I. (1983) in *Spectroscopy and Excitation Dynamics of Condensed Molecular Systems*, eds. Agranovich, V. M. & Hochstrasser, R. M. (North-Holland, Amsterdam), pp. 555–619.

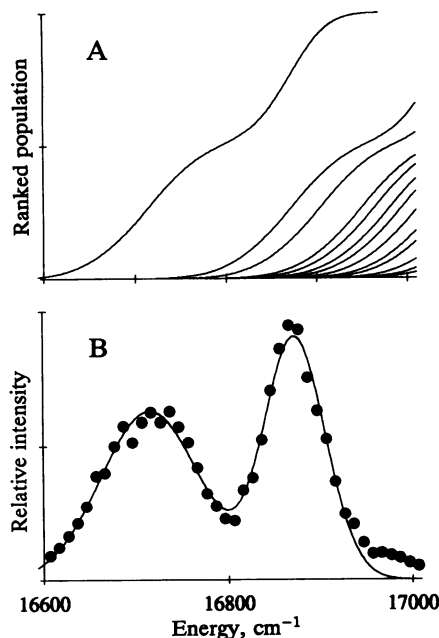


FIG. 4. (A) Part of the vibronic energy map of MgMb. (B) PDF of MgMb.

2. Friedrich, J. & Haarer, D. (1984) *Angew. Chem. Int. Ed. Engl.* **23**, 113–140.
3. Angiolillo, P. J., Leigh, J. S., Jr., & Vanderkooi, J. M. (1982) *Photochem. Photobiol.* **36**, 133–137.
4. Vanderkooi, J. M., Moy, V. T., Maniara, G. & Koloczek, H. (1985) *Biochemistry* **24**, 7931–7935.
5. Koloczek, H., Fidy, J. & Vanderkooi, J. M. (1987) *J. Chem. Phys.* **87**, 4388–4394.
6. Holtom, G. R., Trommsdorff, H. P. & Hochstrasser, R. M. (1986) *Chem. Phys. Lett.* **131**, 44–50.
7. Kohler, B. E. (1979) in *Chemical and Biochemical Applications of Lasers*, ed. Moore, C. B. (Academic, New York), pp. 31–51.
8. Kaposi, A. D., Logovinsky, V. & Vanderkooi, J. M. (1992) *Proc. Soc. Photo-Opt. Instrum. Eng.* **1640**, 792–799.
9. Fuenfschilling, J. & Zschokke-Graenacher, I. (1982) *Chem. Phys. Lett.* **91**, 122–125.
10. Fidy, J., Vanderkooi, J. M., Zollfrank, J. & Friedrich, J. (1992) *Biophys. J.* **61**, 381–391.
11. Jankowiak, R. & Small, G. J. (1989) *Anal. Chem.* **61**, 1023–1032.
12. Fidy, J., Holtom, G. R., Paul, K.-G. & Vanderkooi, J. M. (1991) *J. Phys. Chem.* **95**, 4364–4370.
13. Logovinsky, V., Kaposi, A. D. & Vanderkooi, J. M. (1991) *J. Fluoresc.* **1**, 79–86.
14. Ormos, P., Ansari, A., Braunstein, D., Cowen, B. R., Frauenfelder, H., Hong, M. K., Iben, I. E. T., Sauke, T. B., Steinbach, P. & Young, R. D. (1980) *Biophys. J.* **57**, 191–199.
15. Campbell, B. F., Chance, M. R. & Friedman, J. M. (1987) *Science* **238**, 373–376.